Journal of Crystal Growth 75 (1986) 441–453
North-Holland, Amsterdam

GROWTH HISTORY OF PbS SINGLE CRYSTALS AT ROOM TEMPERATURE

Juan Manuel GARCÍA-RUÍZ

Departamento de Geología, Universidad de Cádiz, Apdo. 40, Puerto Real, Cádiz, Spain

Received 30 July 1985; manuscript received in final form 28 February 1986

The growth history of PbS single crystals in silica gels acidified with HCl and $HClO_4$ has been studied. A morphological evolution from dendritic growth (along {100} in HCl medium and {111} in $HClO_4$ medium) to single crystals with equilibrium shape has been observed. The morphogenetical process is related to the growth mechanism dominating at different growth stages. This explanation agrees with the change of supersaturation expected in diffusing-reacting systems and with the surface topography analysis carried out by scanning electron microscopy.

1. Introduction

Galena, lead sulphide with halite-type structure, is the most important lead mineral in the earth's crust. Apart form the lead content, recoverable amounts of Bi, Ag, Cu, etc. are usually present. PbS is further interesting because it is a naturally occurring semiconductor [1]; indeed, transistor action has been demonstrated in some of the purest specimens [2].

Blank and co-workers [3–5] and Sangwal and Patel [6] have described the growth of PbS single crystals at room temperature. They used a test tube variant of the gel technique and used an acidified medium with HCl to pH 6 [6] or lower [3–5]. In a previous paper [7], the present author has reported the growth of PbS single crystals by using U-tubes and a $HClO_4$ medium which leads to large crystal size. During these experiments, it was observed that most of the growth process occurs in the instability region and after further growth, the equilibrium morphology was obtained. Therefore it was thought worthwhile to study carefully the morphological growth process of PbS crystals at room temperature, which can give reliable information on the fields of both, mineral genesis and growth of crystals.

This paper deals with the growth behavior of PbS single crystals by the counter-diffusion variant, using gel media acidified with HCl or $HClO_4$. The morphology of the crystals was monitored in situ by optical microscopy. Some crystals were recovered from the gel, and their surface topography was observed by scanning electron microscopy. An evolution from instability to equilibrium was found via two different dendritic patterns which depend on the growth medium. An explanation of this evolution is presented, which is supported by crystal surface analysis and the present state of the theory of crystal growth in diffusing-reacting systems.

2. Experimental procedure

Previous studies were carried out by using a two-layer method in test tubes in a manner similar to that reported by Blank et al. [3] and Blank and Brenner [4]. A three-layer method was also investigated. However, the system has since been improved in terms of crystal size, nucleation density and ease of observation, by employing a U-tube arrangement. The results reported below, therefore, refer only to the last technique.

The U-tubes employed provided three different diffusion path lengths: 80 mm, 140 mm and 280 mm. The horizontal part of the U-tube was filled with silica gel produced by the acidification of a Na_2SiO_3 solution (Merck, sp.gr.: 1.059 g/cm^3; pH 11.2) with a HCl (3N) or $HClO_4$ (3N) solution

0022-0248/86/$03.50

until the desired pH was obtained. Gelling time is pH dependent, being about 100 h for pH 2 and 125 h for pH 1.3. The two reactant solutions were poured on the vertical branches of the U-tube. An organic sulphur compound, thioacetamide (Merck analytic grade), was employed as the sulphide ion donor because, as Blank et al. [3] pointed out, the use of this compound makes available only a limited amount of S^{2-} ions at any time. This avoids an excessive PbS supersaturation and consequent polycrystalline nucleation. As lead donors, $Pb(NO_3)_2$ or $Pb(NO_3)_2$ previously complexed with Na–EDTA were used, always in doubly distilled water. Thus, the chemical reactions implied were:

$$Ch_2CSNH_2 \overset{H_2O}{\rightleftharpoons} S^{2-} + CH_3CONH_2, \quad (1)$$

$$Pb(NO_3)_2 \overset{H_2O}{\rightleftharpoons} Pb^{2+} 2\,NO_3^{2-}, \quad (2)$$

$$Pb(NO_3)_2 + Na_2\text{–EDTA} \overset{H^+}{\rightleftharpoons} Pb^{2+} + 2\,NaNO_3 + H\text{–EDTA}, \quad (3)$$

$$Pb^{2+} + S^{2-} \rightleftharpoons PbS. \quad (4)$$

All the experiments were conducted at room temperature. In some cases a hybrid gel technique was used, a variation in which crystals are grown in a gel-free zone situated in the middle of the U-tube [8]. The evolution of the crystal morphology was monitored daily by transmission optical microscope and binocular lens. The crystals were recovered by dissolving the silica gel with sodium hydroxide (1N) and mechanical manipulation. They were then washed with distilled water and alcohol until free of all silica gel under microscopic inspection.

Identification was made by chemical analysis and X-ray diffraction (single crystal and powder methods with filtered Cu Kα radiation). The morphology and surface structures of PbS were studied by optical microscopy (OM) and scanning electron microscopy (SEM). For the SEM studies, the crystals were fixed on Al bases. Gold metallization was subsequently applied.

3. Results

3.1. Identification

The experiments begun ($t = 0$) by placing the reactant solutions in the two branches of the U-tube. The induction time t_i, i.e., the time taken for the first crystallites to appear under magnification $\times 500$, is related to the diffusion path length, being 4 days for $L = 80$ mm, 9 days for $L = 140$ mm and 25 days for $L = 280$ mm; t_i is related to the nucleation time, which cannot be directly measured from the experiments. After these values of t_i, some crystals appeared, which had a steel-gray color and a strong metallic lustre; they were identified as galena by X-ray diffraction. Spectrophotometric techniques [7] showed them to be of high purity, in agreement with the results of Blank et al. [3]. Within $t = 40$–50 days, some large and transparent single or twinned crystals appeared, which were identified by X-ray diffraction as ethylenediaminetetraacetic acid (EDTA), a byproduct formed after reaction [3]. In those cases where the growth period was further prolonged, such crystals attained larger sizes ($= 15$ mm), sometimes even growing around the PbS crystals previously formed, and ocluding them.

3.2. Crystal morphology

According to earlier experiments [3–7], PbS single crystals grow in silica gel in the form of cubes {100}, and cubo-octahedra {100} and {111}. Dodecahedron {110} and pyritohedron {210} forms were not found. Twinned crystals have also been observed in some cases, and close to the cation branches of the U-tubes nearly spherical crystals are formed by repeated twinning on (111). However, it is important to note that the above-cited forms (cubes and cubo-octahedra) belong only to the final growth stage. An advantage of the gel method is that crystals can be observed in all stages of their growth. Our observation during the experiments clearly shows that a morphological evolution from skeletal and dendritic crystals to the above-mentioned forms, especially to cubes {100}, occurs. It is also worth noting that for all the initial values of gel pH investigated, the mor-

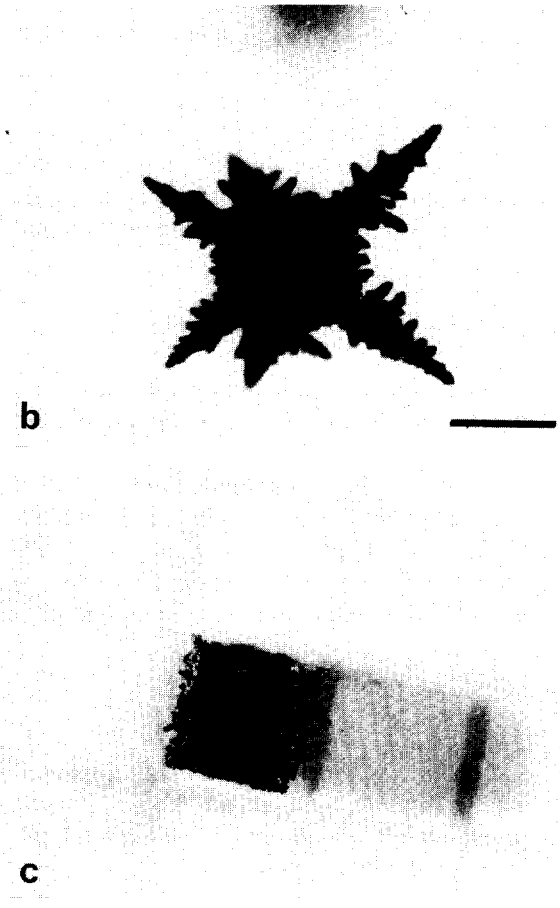

Fig. 1. Optical micrographies showing three different stages of the PbS single crystals growing in silica gels acidified with $HClO_4$. Scale bar in (a) and (b) 0.3 mm; in (c) 1 mm.

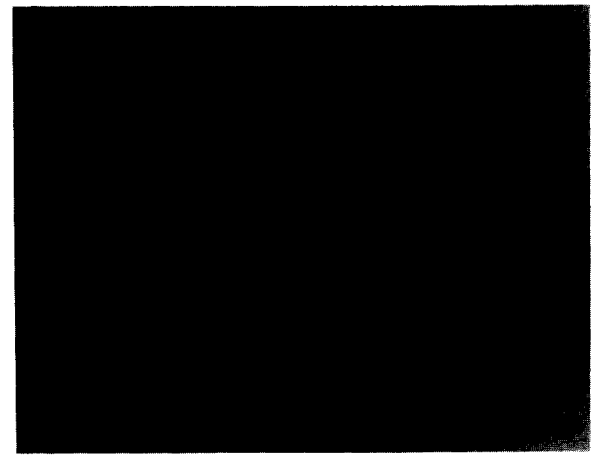

Fig. 2. Optical micrographies showing different growth stages found in PbS crystal obtained in silica gels acidified with HCl. Scale bar in (a) and (b) 0.5 mm; in (c) 1 mm.

phogenetical mechanism of the equilibrium form is related to the growth medium (HCl or $HClO_4$).

3.2.1. Growth in $HClO_4$ medium

When the sodium silicate solutions are acidified with $HClO_4$, the resulting PbS crystals show a tendency to nucleate in the form of dendrites, with overgrowth at the corner of the cube giving morphologies along {111} (fig. 1a). Thus, an eight-branched crystal is formed. Then, the open spaces between the branches are filled by growth along the cube edges and, in this way, hopper crystals are formed, as shown in fig. 1b. With time, crystals take the cube form, with non-flat wavy faces, the center of the faces being slightly depressed (fig. 1c).

3.2.2. Growth in HCl medium

When the sodium metasilicate solution is acidified with HCl, a very different but also interesting growth sequence can be seen. In the early growth stages, one can also observe dendritic growth, but this time along the cube directions {100} (fig. 2a), in such a way that six-branched dendrites are formed. Afterwards, the tips of the branches experience a development along the other two {100} directions, giving the "hypercube" morphology shown in fig. 2b. As a result of the growth process, the morphology of the six-branched skeletons evolve, until cube or cube-octahedral forms occur, as shown in fig. 2c.

4. Discussion

4.1. Theoretical morphology of PbS

The atomic arrangement of galena is the same as that of NaCl, i.e., cubic closed-packed, with Pb atoms in the octahedral interstices [9]. If a Born ionic model is assumed for galena [10] a periodic bond chain (PBC) analysis of crystal morphology gives similar results as those for the NaCl case [11]. Thus, the strongest bonds are found between two adjacent ions, Pb and S, considered as point charges. Although no difference between the attachment energies of Na and Cl exists, only three PBC vectors are found, namely $[\frac{1}{2}00]$, $[0\frac{1}{2}0]$ and $[00\frac{1}{2}]$. The addition of PBC vectors gives the S_1-form {110} and S_2-form {210}. However, the stability of profiles of the (210) face may be more important than the (110), because profile periods or {110} are doubled. The octahedron K-form {111} presents also a doubled profile period. However, Hartman [11] considers (111) as the K-face with the smaller growth rate, due to the influence of the solvent.

Krebs [12] considers that partial covalence prevails in galena by the admixture of lead 6p orbitals into the sulfur 3p orbitals. Therefore, if a covalent bond model is assumed, then the {110} S-form has the simplest profile and, consequently, should be morphologically more important than the {210} S-form. The profile of the octahedron face is also the smallest possible, and the growth rate along {111} should be considerably higher than in the ionic model. Therefore, the results described above in section 3.2 show that in PbS single crystals grown by diffusion in silica gel, a clear tendency to equilibrium morphology exists in both HCl and $HClO_4$ media.

4.2 Morphological evolution of PbS crystals

The tendency to the equilibrium shape observed in the growth of PbS crystals is expected, when considering the kinetics aspects of crystal growth by diffusion. In previous papers [13,8] it has been demonstrated that the rate at which the ionic concentration product (π_{AB}) grows at the point where the nucleation takes place can be obtained from the expression:

$$\pi_{AB} = C_{0A}^2 C_{0B} \operatorname{erfc}^2\left(\frac{L}{2\sqrt{t}\left(\sqrt{D_A}+\sqrt{D_B}\right)}\right), \qquad (5)$$

where C_{0A} and C_{0B} are the initial concentrations of the reactants, D_A and D_B are their diffusion coefficients, erfc is the inverse Gauss error function, and t is the time.

Fig. 3 is a plot of a typical case, showing the increment of the ionic concentration product versus time from a computer experiment. C_A and C_B being equals for all the t values, the nucleation will occur when $\pi_{AB} = K_n$, where K_n is the ionic concentration product for nucleation. Let us

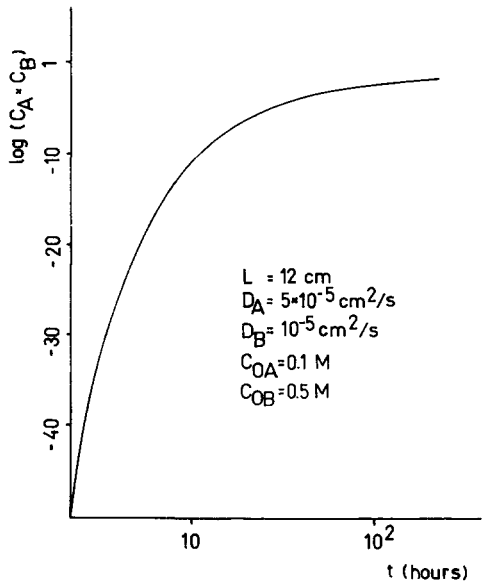

Fig. 3. The rate of development of concentration in the point where the first precipitate will appear.

now consider the case of PbS, a compound with a solubility product, K_s, of the order of 10^{-28}; K_n will therefore be some orders of magnitude higher. In accord with fig. 3, K_n will be overtaken by π_{AB} in the lower part of the curve, where the development rate of the supersaturation ratio is $\sigma = \pi_{AB}/K_s$.

As a consequence, nucleation as well as the earlier growth stages of the PbS crystals would be situated in the instability region of the qualitative Sunagawa model [14] (see fig. 4). Therefore, from the nucleation stage to a certain critical supersaturation σ^{**}, the dominant mechanism is continuous three-dimensional (3D) surface nucleation growth and, in accordance with theory, a dendritic array is expected to arise. Then, as a result of the precipitation process, the supersaturation will decay towards the equilibrium concentration. When obtaining precipitates of insoluble substances (such as PbS) by rapidly mixing two solutions (for instance, thioacetamide and lead nitrate), the equilibrium concentration is soon attained, and the precipitate is "quenched" without later morphological evolution (disregarding Ostwald ripening phenomena at long range time).

In contrast, the present case of growth in gels deals with a non-homogeneous system in which macroscopic concentration gradients exist. Then, once the first precipitate is formed, new reactants are continuously arriving at the site. The exact pattern of the incoming flux depends on the diffusion coefficients, the concentrations, the values of K_s and K_n, and the length of the gel column [15]. As a general rule, the growth rate of the supersaturation will decrease continuously in such a way that PbS crystals enter into the growth region where the growth rate is controlled by the two-dimensional (2D) nucleation mechanism proposed by Kossel and Stranski (KS) [16], where hopper crystals are expected to occur. Finally, growth is controlled by screw dislocations, by the mechanism of Burton, Cabrera and Frank (BCF) theory [17], giving polyhedral crystals. It should be noted that, according to the analysis of Kuroda et al. [18], this transition from the continuous growth to the KS and BCF growth mechanisms is accelerated by the increasing size of the crystals. Therefore, it is suggested that the growth of PbS single crystals by diffusion transport at room temperature is successively controlled by three different mechanisms, as shown by the arrow in fig. 4.

The morphological evolution patterns found in the experimental results described above are in agreement with this argument. Also, more evidence for this interpretation can be obtained by a careful analysis of the surface microphotography of crystals belonging to different growth stages of the morphological sequence. As the early dendritic pattern belonging to each growth medium (HCl and $HClO_4$) imposes two different morphological evolutions, we will analyze each of them separately in the following sections.

4.2.1. Surface topography of PbS crystals grown in $HClO_4$ medium

The morphological sequence of the PbS crystals growing in $HClO_4$ medium, i.e., dendritic growth along {111} → hopper {100} faces → polyhedral crystal with equilibrium morphology, is that expected from PBC analysis. Fig. 5a shows a [010] view of a PbS dendrite cut in half. Three generations of branches are observed. The tip angle was 60° and the axial angle found was 70°, i.e., similar to the angle between the preferred growth {111}

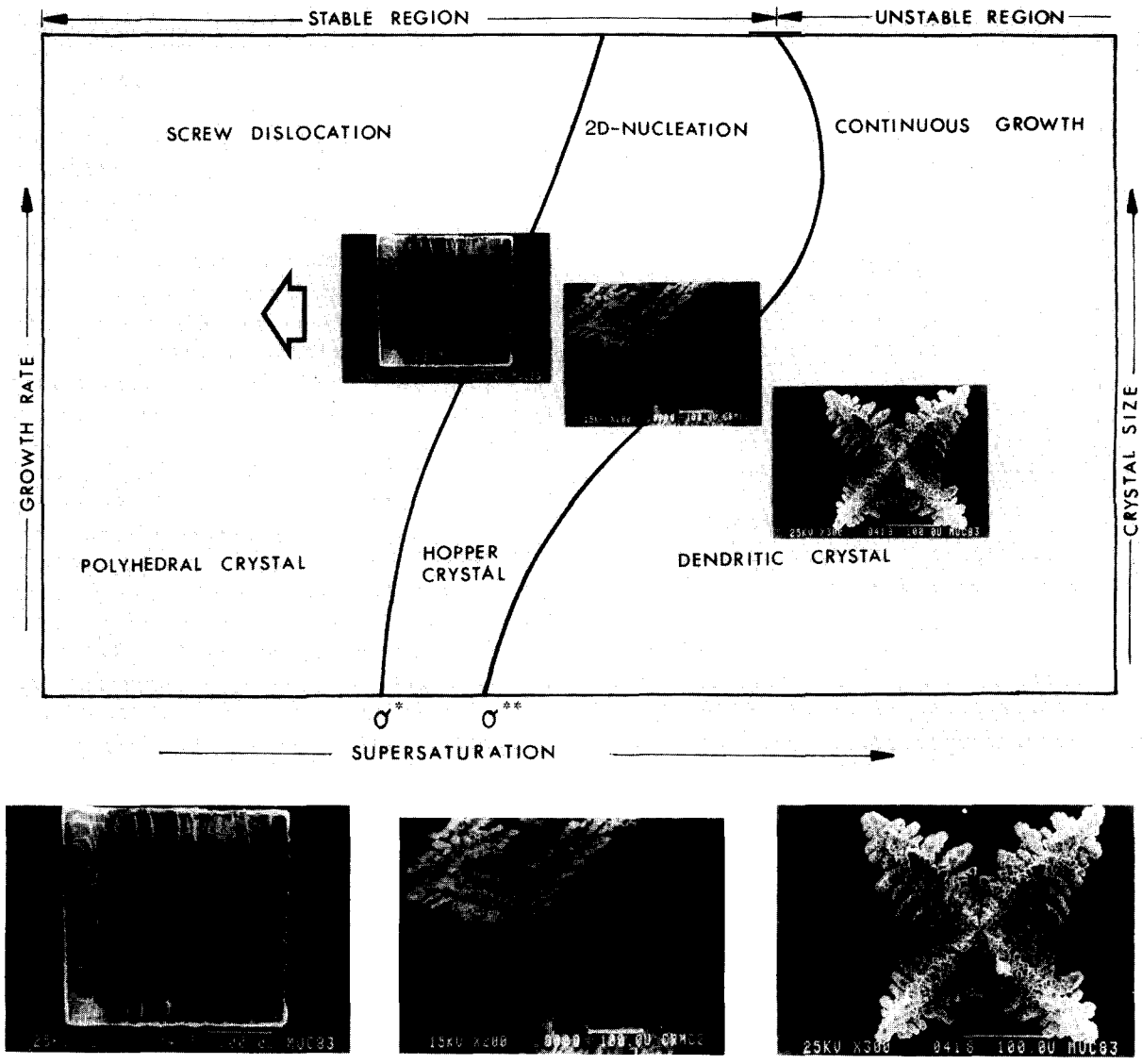

Fig. 4. Top: A supersaturation versus crystal size diagram (see ref. [14]) showing the growth evolution of PbS crystals growing in gels and the three dominating growth mechanisms. Bottom: Enlarged views of the crystals.

directions. These branches consist of small crystallites, with sizes varying from 0.5 μm in the zone nearer to the core, to 10 μm in the tip of the primary branches. These crystallites show {100}, {110} and {111} faces and, as their size increases, only (100) faces, i.e., the equilibrium shape begins to dominate the morphology.

Fig. 5b shows one of the branches belonging to an evolving dendrite. Note again the relation between crystal size versus distance from the core, and the fact that the crystals on the tips already show hopper faces, suggesting that two-dimensional nucleation is already the main growth mechanism. This is clearer in fig. 6a, which shows a SEM view of a typical hopper crystal. At higher magnification (fig. 6b) one can observe clusters of

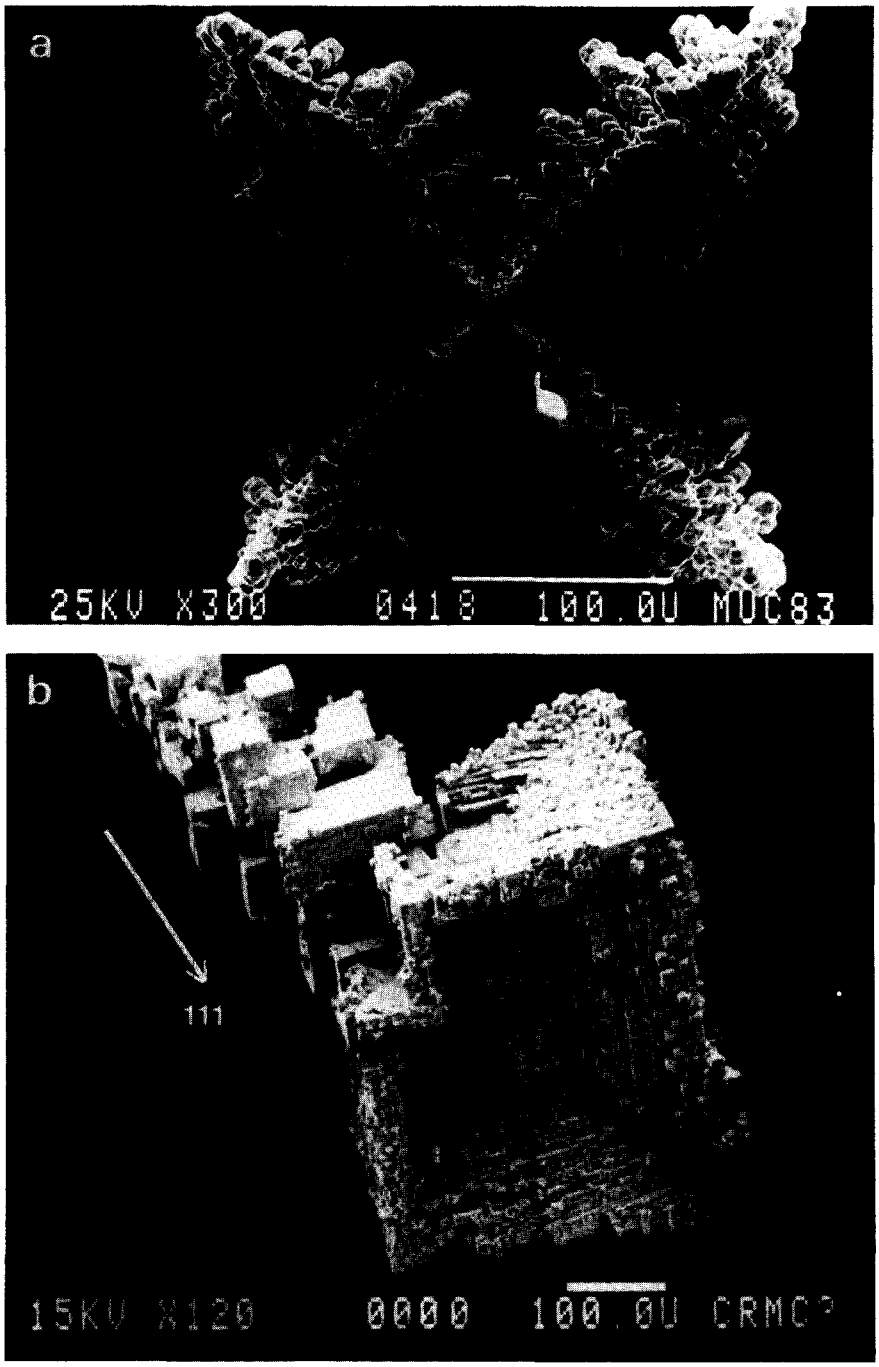

Fig. 5. (a) Dendritic growth along [111] in PbS single crystals growing in $HClO_4$ medium. (b) A dendritic arm beloning to a evolver crystal; arrow shows growth directions.

1 μm edge size – about 2000 (010) layers – on the crystal surfaces. The smaller nuclei show {100} and {110} faces, but on the larger ones the {110} faces disappear because of their higher growth rate.

In some of these nuclei with an edge length

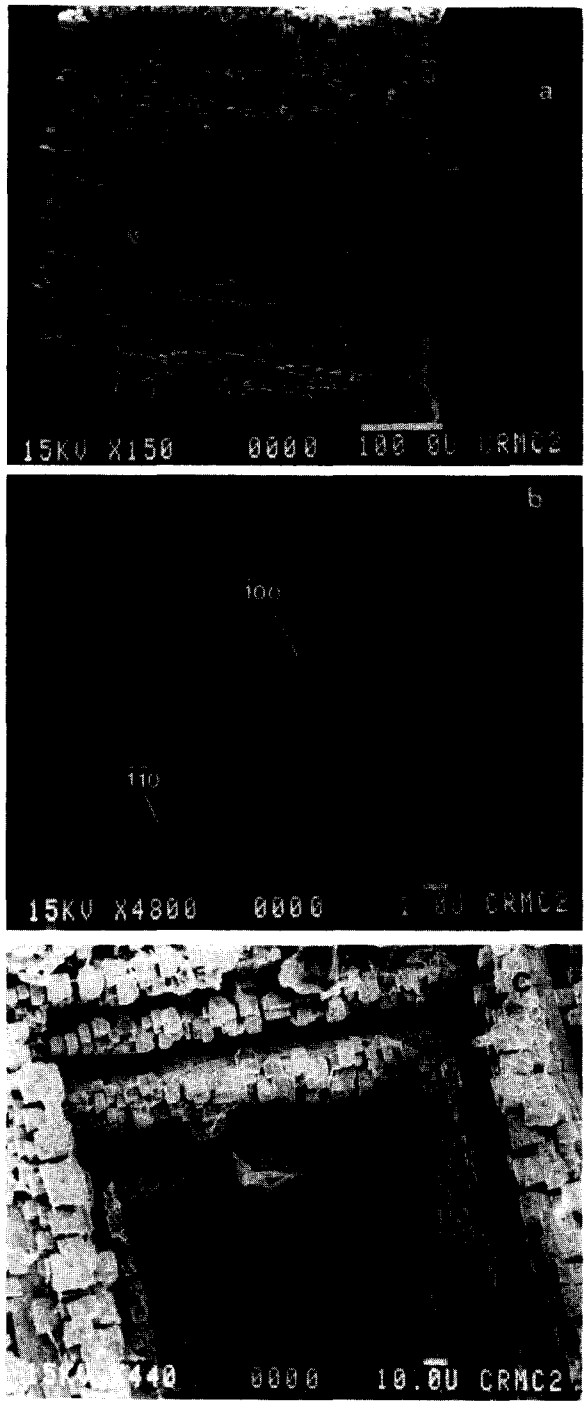

Fig. 6. (a) Hopper crystal of PbS. (b) Surface nucleation on a {100} face of a PbS crystal with surface nuclei showing {100} and {110} faces. See text.

larger than 2.5×10^4 Å, the hopper core can be clearly seen, which suggests that the Berg effect [19] is also present as in the whole face. The topography of the evolved hopper face in fig. 6c shows the surface to be built by a large number of nuclei with an average size of 20 μm. It suggests that the spread of 2D nuclei is not the main process of filling the surface, and that nucleation occurs by the attachment of block nuclei. This mechanism was inferred by Glasner and Tassa [20] for the case of KCl crystal grown from solution. The stacking of block nuclei dominating the spread rate of growth layers could explain the misorientation between block nuclei observed, sometimes with a value of 12°. This misorentation imposes the surface topography observed after further growth into the 2D growth region, when

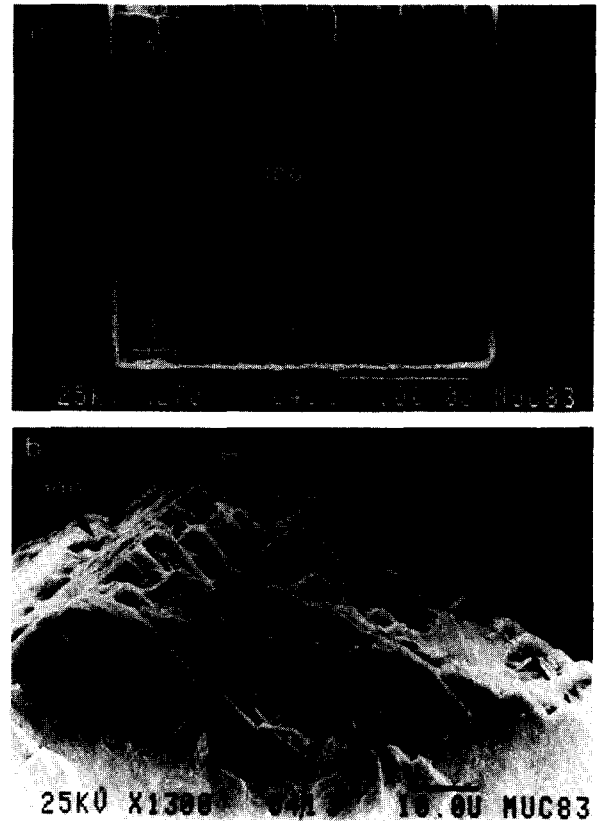

Fig. 7. (a) A later stage of the PbS crystal showing lineage texture. (b) The K-surface of the {111} faces.

the crystal approaches the equilibrium morphology and the existence of the so-called lineage texture [21].

Fig. 7a shows such a texture on a cubic single crystal with slightly concave {100} faces. As predicted from the PBC analysis, the octahedral (111) faces are K-faces. In fig. 7b the kink surface microtopography of {111} faces at later stages of its existence can be observed. No evidence of screw-dislocation growth has been clearly found on the crystal surfaces. Thus, for the length of time of the experiment ($\simeq 40$ days) the process has been stopped in the KS region. However, the next growth stage is expected to be in the BCF region, as shown by the arrow in fig. 4.

The fact that dissolution–precipitation phenomena due to the effect of surface tension on the interfaces have not been observed by microscopy and the evidence shown by the surface analysis lead one to the conclusion that the change of shape leading to the theoretical morphology observed in PbS crystals grown in $HClO_4$ medium is related to the growth mechanism dominating at different supersaturation values. This, in turn, supports the theoretical model of crystal growth by the diffusion mechanism used here.

4.2.2. Surface topography of PbS crystals grown in HCl medium

The results obtained in the case of PbS crystals grown in HCl medium are also consistent with the arguments discussed in section 4.2.1, but in this case the morphological evolution imposed by the dendritic pattern is quite different. Fig. 8b shows

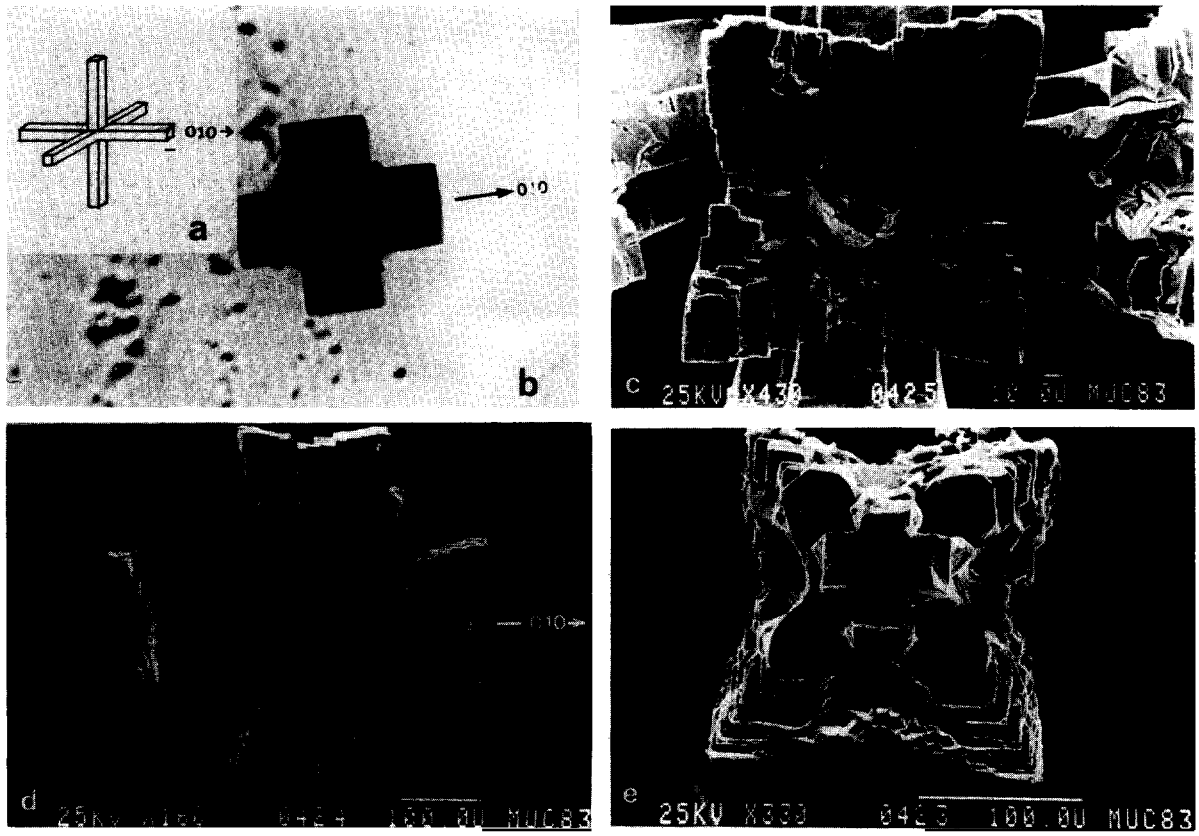

Fig. 8. Dendritic growth along {100} in PbS crystals grown in HCl medium; (e) is a view from the core of a [010] dendritic branche. See text.

the dendritic morpholgy coming from the postulated skeleton crystal diagramatically shown in fig. 8a (see also fig. 2b). A six-branched pattern is observed with preferred growth along {100}, i.e., normal to the {100} F-faces. The secondary family of branches grow along directions perpendicular to the stem. Each secondary family appears to be a continuous structure, perhaps because the interdendritic arm spacing of the third order family is very small and after further growth it is rapidly filled (see fig. 8c). Thus, the section normal to the first-order dendrites is cross-shaped. After a certain critical size, the preferred growth directions change drastically from {100} to {111}. Therefore, the top of each branch of the stem present now four ([111], [1$\bar{1}$1], [$\bar{1}$11] and [$\bar{1}\bar{1}$1]) main directions of development, the other four directions of the {111} set being retarded by geometry. This explains the overall morphology observed in fig. 8d. Fig. 8e shows a similar dendrite cut in half. At the center, the cross-shaped section of the stem can be observed, and in the outer part, the morphology obtained by preferred growth along {111} can be clearly distinguished. Note that as the growth progresses, the {111} faces on the crystallites, which form the dendrite disappear.

After further growth in this stage a cube-like crystal with face centered plateau is formed, as shown in fig. 9a. The plateau on each cube face shows growth layers with macro-step heights, in such a way that the plateau centers are slightly depressed (fig. 9b). The empty space belonging to the position of an ideal octahedral face is shown in fig. 9c. Note that all the corners on the dendrite show triangular {111} faces, but the edges are sharp and no trace of dodecahedral faces is pre-

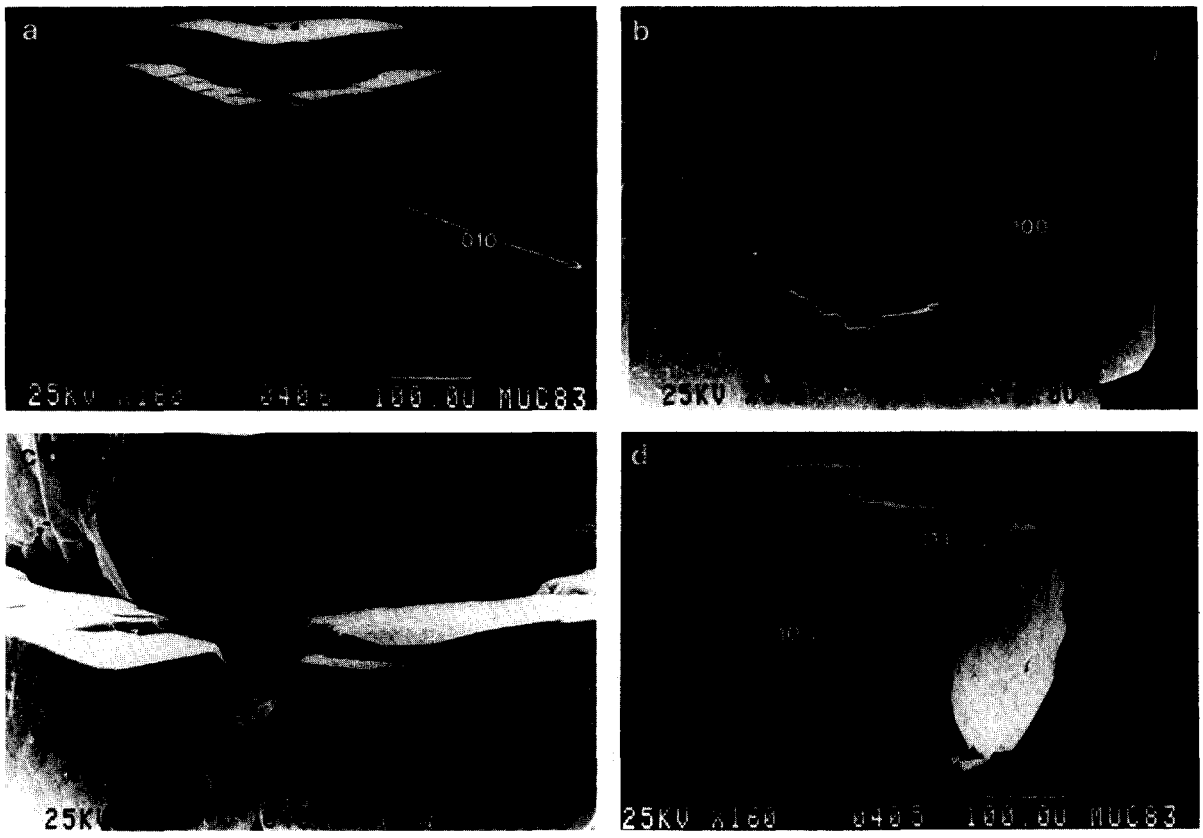

Fig. 9. The transition from dendritic growth along [100] to cube form in PbS grown in HCl medium.

sent. This explains the next morphological step observed (fig. 9d), where one can distinguish {100} and {111} faces, the {110} edges presenting serrated profiles by the presence of {111} surfaces.

The absence of stepped dodecahedral faces suggests the inability for 2D nucleation and the spread of growth layers on F-faces, the main growth mechanism being the nucleation on {111} faces. This is best illustrated on fig. 10a, in which a crystal belonging to a further growth step is shown. Here a cubo-octahedron form with smooth {100} faces and rough {111} surfaces is shown. The block nuclei building octahedral faces present clear {111} surfaces, and it seems that the growth continues by stacking of blocks on the {111} surfaces (fig. 10b). Note the differences between this case and the case of PbS crystal grown in $HClO_4$, where the topography of the {111} faces is drastically different.

Birchall and Davey [22] have described the formation of skeleton crystals along the {100} directions, and centered plateaus on cube faces in NaCl (isostructural with PbS) crystals, grown from solutions in the presence of sodium alginate (SA) and λ and K carragheens. These authors explain the phenomenon as due to step bunching resulting from the preferential polysaccharide adsorption at the edges, which retard the developement of edge nuclei. In the present case of PbS growth in HCl medium, it seems also plausible to attribute the observed behavior to an impurity effect. In fact, all the previous work on PbS single crystals grown in silica gel was carried out in HCl acidified gel [2–6], varying the pH, lead donor solutions and temperature. The most comprehensive treatment was given by Sangwal and Patel [6]. Although some of the conclusions inferred by these authors are inconsistent with our results (specifically the assertions that (a) the growth proceeds by successive deposition of the material on cube faces only, (b) large amounts of gel are included by PbS crystals during growth, and (c) at later growth stages {100} faces developed further than {111}), their results can be reinterpreted in agreement with the explanation proposed here. Sangwal and Patel describe the larger growth rate on {100} to be a consequence of the adsorption of acetamide, forming from the hydrolysis of the thioacetamide

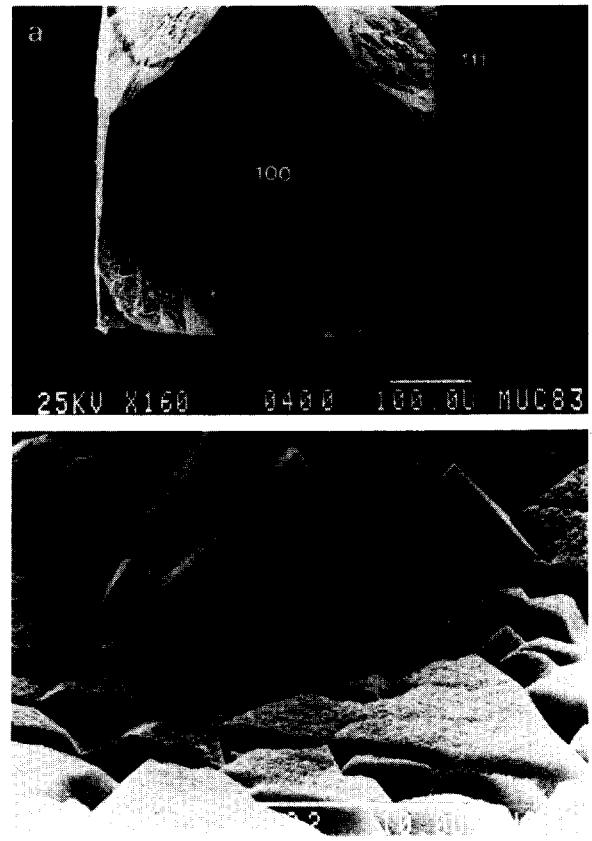

Fig. 10. The K-surface of the {111} faces in PbS crystals grown in HCl medium.

(reaction (3)). However, the same S^{2-} ion donor is used in the case of PbS growth in $HClO_4$ medium resulting in the dendritic pattern, as theoretically expected. Further work on this point must be performed to elucidate the effect of impurities.

5. Further considerations

The morphogenetical pattern recorded in this study leads one to consider the use of crystal growth in porous media as a technique for obtaining experimentally the equilibrium shape of the crystals. In this technique, diffusion in the solution bulk has been demonstrated to be the rate-determining step of the growth process which occurs under isothermal conditions. In our experimental arrangement, an initial macroscopic concentration

gradient is imposed on the system which later evolves toward equilibrium. However, the process of morphological change described here is clearly different from those discussed in the classical method by Lemlein and Kliya [23,24], because in gel growth, the place where the crystals actually grow must be considered as an open thermodynamic system. Consequently, according to the experimental data during the process leading to the minimum surface energy of the growing crystals, their volume is not constant. Thus, as discussed above, we must emphasize that the change of morphology observed in PbS single crystals growing in gels is a reflex of the dominant growth mechanism.

However, one can expect a spontaneous change of shape using the technique of growth in gels if two requeriments are satisfied:

(1) Lack of macroscopic gradients, which can be obtained by (a) using experimental arrangements ad hoc, or (b) using the classical ones, once the macroscopic homogeneity of the system has been achieved. In fact, these reorganization phenomena have been observed at large experimental times, in the case of KDP and $LiIO_3$ crystals growing in TMS gels [25].

(2) The use of very soluble compounds. According to Chernov [26], the characteristic time of transformation t_T to an equilibrium shape is estimated to be:

$$t_T \simeq kTR^3/3\Omega^2 DC_e\alpha, \quad (6)$$

where k is the Boltzmann constant, T the temperature, R the nonequilibrium curvature radius, Ω the atomic volume, C_e the equilibrium concentration and α the specific free-surface energy. This author shows that t_T takes reasonable values for very small ($\simeq 10^{-3}$ cm) crystals but it can be easily derived from relation (6) that t_T is inversely related and highly sensitive to C_e. For instance, in the case of PbS, a very insoluble compound, t_T would be in the range of thousands of years, even for $R = 100$ μm.

The applications of morphogenetical studies, as in the present paper, to mineral genesis problems are evident. It is expected that the morphogenetical process of the crystals must be recorded in its internal structure. In fact, preliminary studies on polished sections of our synthetic galena crystals by using ore microscopy reveals, after etching, different internal heterogeneities. As Sunagawa points out [27], by comparing well-decoded paragenetic records in synthetic crystals with those observed in nature, we will have the key to deciphering the growth history of minerals. As previously proposed [8], crystal growth by the diffusion method appears to be an appropriate technique to this aim.

Acknowledgements

The author gratefully acknowledge useful discussions with Professor H.K. Henisch and the help of Dr. J.M. Gomez de Salazar for the SEM work (those pictures labeled MUC).

References

[1] D.G. Thomas, II–VI Semiconductors (Benjamin, New York, 1967).
[2] P.C. Banbury, H.A. Gebbie and C.A. Hogarth, in: Semiconducting Materials, Ed. H.K. Henisch (Butterworths, London, 1951).
[3] Z. Blank, W. Brenner and Y. Okamoto, Mater. Res. Bull. 3 (1968) 555.
[4] Z. Blank and W. Brenner, J. Crystal Growth 11 (1971) 255.
[5] W. Brenner, Z. Blank and Y. Okamoto, Nature 212 (1966) 392.
[6] K. Sangwal and R. Patel, J. Crystal Growth 23 (1974) 282.
[7] P. Aragón, M.J. Santos, A. Maceira, R. Gallego Andreu and J.M. García-Ruíz, An. Quim. 80 (1984) 134.
[8] J.M. García-Ruíz, in: Crystal Growth in Sedimentary Environments, Eds. R. Rodríguez and I. Sunagawa, Estudios Geol. 38 (1982) 209.
[9] B. Wassertein, Am. Mineralogist 36 (1951) 102.
[10] W.W. Scanlon, Mineral. Soc. Am. Special Paper 1 (1963) 135.
[11] P. Hartman, in: Relations Between Structure and Morphology of Crystals, Thesis, University of Groningen (1953).
[12] H. Krebs, Fundamentals of Inorganic Crystal Chemistry (McGraw-Hill, London, 1968).
[13] J.M. García-Ruíz and F. Míguez, Estudios Geol. 38 (1982) 3.
[14] I. Sunagawa, Bull. Mineral. 104 (1981) 81.
[15] H.K. Henisch and J.M. García-Ruíz, J. Crystal Growth 75 (1986) 195, 203.

[16] I.N. Stranski and R. Kaischew, Usp. Fiz. Nauk 21 (1939) 408.
[17] W.K. Burton, N. Cabrera and F.C. Frank, Phil. Trans. Roy. Soc. London A243 (1951) 299.
[18] T. Kuroda, T. Irisawa and A. Ookawa, J. Crystal Growth 42 (1977) 41.
[19] W.F. Berg, Proc. Roy. Soc. (London) 4164 (1938) 75.
[20] A. Glasner and M. Tassa, Israel J. Chem. 12 (1974) 817, 799.
[21] M.J. Buerger, Am. Mineralogist 17 (1932) 177.
[22] J.D. Birchall and R.J. Davey, J. Crystal Growth 54 (1981) 323.
[23] G.G. Lemlein, Dokl. Akad. Nauk SSSR 98 (1954) 873.
[24] M.O. Kliya, Kristallografiya 1 (1956) 577.
[25] A. Santos and J.M. García-Ruíz, unpublished results.
[26] A.A. Chernov, Modern Crystallography III (Springer, Berlin, 1984).
[27] I. Sunagawa, J. Crystal Growth 42 (1977) 214.